

Methods for correcting morphological-based deficiencies in hyperspectral images of round objects

Ron Haff^{1*}, Sirinnapa Saranwong^{2,3} and Sumio Kawano^{2,4}

¹United States Department of Agriculture, Agricultural Research Service, Western Regional Research Centre, Albany, CA, 95616, USA

²National Food Research Institute, National Agriculture and Food Research Organisation, Tsukuba, 305-8642, Japan

³Present address: Bruker Optics KK, Tokyo, 104-0033, Japan

⁴Present address: Faculty of Agriculture, Kagoshima University, Kagoshima 890-0065, Japan

*Corresponding author: ron.haff@ars.usda.gov

Introduction

Near infrared (NIR) images of curved surfaces contain undesirable artifacts that are a consequence of the morphology of the sample. Figure 1 shows the 800 nm image of a spherical Teflon sample generated on a linescan hyperspectral imaging system. The left and right images are the same, except that selected pixel intensities are set to 0 in the right image to illustrate the pattern of pixel intensities. The dark band at the equator is a strip of black tape, added so that there would be some detail in the image. The graph on the right shows the pixel intensity along a cross-section of the image. A variety of approaches are reported to address the morphological-based deficiencies, including chemometric pre-treatments combined with principal component analysis,¹⁻⁴ normalisation and averaging along vertical and horizontal intensity curves,⁵ ellipsoidal surface fitting and morphological shrinking.⁶

The objective here is to develop a software correction to remove the variation in pixel intensity based directly on well-known physical effects involving light reflection and intensity. The ideal result would be a uniform image (as is appropriate for a uniform sample). The three predominant principles investigated are described below.

Theory

Diffuse internal reflection and Lambert's law

Reflections of light from surfaces generally exhibit either Lambertian reflection (diffuse internal reflection) or specular reflection. The latter describes reflection from smooth surfaces such as mirrors, glass, or water. Most objects in nature behave primarily as Lambertian surfaces and reflect light through diffuse internal reflection. Thus, the light reflected from Lambertian surfaces has travelled inside the sample and contains information about the interior of the sample. In specular reflection, on the other hand, light reflects directly off the surface of the sample, with the angle of reflection being equal to the angle of incidence. Here we assume the sample is a Lambertian surface and derive the equations to remove the consequences of this from the images.

$1/R^2$ pixel intensity dependence

When imaging flat samples, the difference in pathlength that the light must travel from the sample to the detector is very small between different parts of the sample. When considerable depth is introduced, as in the case of a spherical sample, this is no longer the case. The increased distance travelled by the light from the edge of the sphere versus that at the centre in fact introduces a significant variation in pixel intensity. A correction for this variation was derived and applied to the images.

Variation in arc length along the sample surface as seen by the detector

Figure 2 shows the cross-section of a slice of the sample as imaged by the linescan camera at a particular instance. From the point of view of the camera, the surface is divided equally and each detector measures light intensity over an equal area. Because of the curvature of the sample, however, there are different surface areas contributing at different points along the scan line. A correction for this variation was also derived and applied to the images.

The three corrections described above were combined and applied to the images to test the efficacy of correcting the morphological based deficiencies.

Reference paper as:

Haff, R., Saranwong, S. and Kawano, S. (2012). Methods for correcting morphological-based deficiencies in hyperspectral images of round objects, in: Proceedings of the 15th International Conference on Near Infrared Spectroscopy, Edited by M. Manley, C.M. McGovern, D.B. Thomas and G. Downey, Cape Town, South Africa, pp. 48-51.

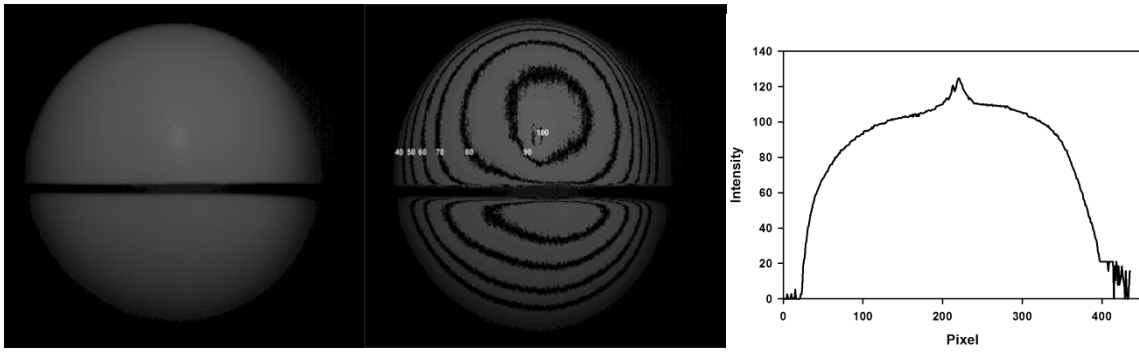


Figure 1. NIR image (800 nm) of spherical Teflon sample (left and centre) and plot of pixel intensity across the sample. Selected pixel intensities are set to 0 in the center image to illustrate the pattern of pixel intensities.

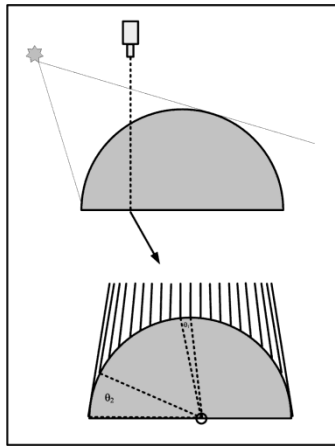


Figure 2. As the sample travels below the camera (top), it is imaged one line at a time (bottom). The curvature of the sample causes larger arc lengths to contribute to pixel intensities towards the edge of the sample.

Materials and Methods

Hyperspectral images from 700 to 1000 nm of a spherical Teflon sample (10 cm diameter) were generated using a linescan hyperspectral imaging system described in previous work.⁷ A C program was developed to strip the bitmap headers from the images and load the intensity data into arrays for application of correction algorithms. The camera/sample system was represented in spherical coordinates (Figure 3) with the origin at the centre of the sample and the z axis along the direction of travel of the sample. Arrays were generated containing the values of the angles θ_1 and θ_2 at each pixel location in the image, thus allowing derived correction algorithms to be applied to the images. The corrections for the three effects were derived and applied as follows.

Lambertian reflection

Lambertian surfaces reflect light with equal intensity in all directions. The value of this intensity depends on the cosine of the angle between the unit normal vector at the point of reflection and a unit vector along the direction from the origin to the light source. For unit vectors, the cosine of the angle equals the dot product of the two unit vectors. Thus, the maximum intensity occurs at the point on the surface of the sample where the normal vector is pointing directly at the light source. Figure 3 shows the vectors used to derive Equation 1 for the dot product of the two vectors over the surface of the sample. The correction, which will be a value between zero and one for each pixel location, is divided into each intensity value to remove the effect:

$$\hat{p} \cdot \hat{q} = \frac{-R + P_1 \sin \theta \sin \phi + (z' + P_2) \cos \theta}{\sqrt{R^2 + P_1^2 - 2R P_1 \sin \theta \sin \phi + (z' + P_2)^2 - 2R(z' + P_2) \cos \theta}} \quad (1)$$

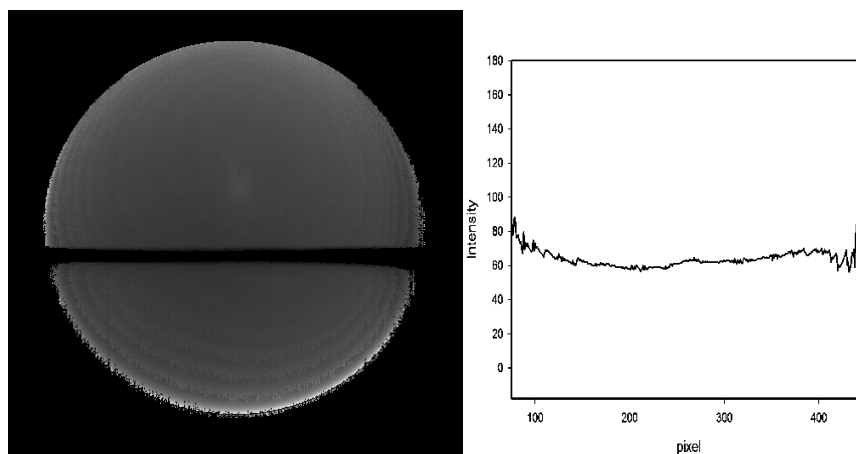


Figure 4. Image of Teflon sphere (800 nm) after correction. Neglecting effects at the outer edge, pixel intensity variation was reduced from 110/255 to 18/255.

A second assumption in the derivations was that of a single light source. While the experimental setup for imaging did employ a single lamp, unintended ambient light and reflections from surfaces also contributed to the intensity distribution as seen at the detector and become a source of error in the calculations. Attempting to calculate the effect of unwanted reflections would be impractical at best and care should be taken to eliminate ambient light and reflections in the imaging setup. Finally, calculations assume full vision of the semi-circle as seen from detector which of course was not the case due to line of sight issues. This leads to small errors in the corrections that result in undesirable effects which become large at pixels along the edge of image. This effect, combined with the problem of unknown arc length at the outermost pixel along the edge, makes the results of applying corrections along the outer edge of the image unpredictable. It would therefore be advisable to mask the edge (set the outermost pixels to zero intensity) to avoid these issues. For real world inspection scenarios this would not be a problem as full surface imaging of a sphere requires three cameras and the outer pixels overlap.

The corrections derived here apply to samples of spherical morphology which apply (approximately) to many agricultural commodities. Many other commodities, such as bananas and cucumbers, have approximately circular cross-sections along a particular axis and the adaptation of the corrections is straightforward.

Conclusion

NIR imaging has potential for quality based inspection of many agricultural products. However, in imaging fruits and vegetables, the sample morphology, i.e. the sample curvature, generates undesirable characteristics in the images that can interfere with the ability to perform the desired inspections. A software correction was developed for images of a Teflon sphere that attempts to remove the effects of sample morphology based on physical principles that describe the reflection and intensity of light under the conditions in question. Pixel intensity variation along a horizontal slice of the image was reduced from 43% to 7%. The same principle can be applied to samples with circular cross-sections along a particular axis, including many agricultural commodities.

References

1. C. Esquerre, A.A. Gowen, C.P. O'Donnell, J. Burger and G. Downey, in *Near Infrared Spectroscopy: Proceedings of the 14th International Conference*, Ed by S. Saranwong, S. Kasemsumran, W. Thanapase and P. Williams, IM Publications, Chichester, UK, pp. 953-957 (2010).
2. J. Xing, C. Bravo, P.T. Jancsó, H. Ramon and J.D. Baerdemaeker, *Biosyst. Eng.* **90**, 27-36 (2005).
3. E. Gaston, J.M. Frías, P.J. Cullen, C.P. O'Donnell and A.A. Gowen, *J. Agric. Food Chem.* **58**, 6226-6233 (2010).
4. P.M. Mehl, Y.R. Chen, M. Kim and D.E. Chan, *J. Food Eng.* **61**, 67-81 (2004).
5. W. Wang and J. Paliwal, *ASAE Annual International Meeting* [Paper Number 053070] (2005).
6. A. Vogel, V.V. Chernomordik, J.D. Riley, M. Hassan, F. Amyot, B. Dasgeb, S.G. Demos, R. Pursley, R.F. Little, R. Yarchoan, Y. Tao and A.H. Gandjbakhche, *J. Biomed. Opt.* **12**, 051604 (2007).
7. S. Saranwong, R.P. Haff, W. Thanapase, A. Janhira, S. Kasemsumran and S. Kawano, *J. Near Infrared Spectrosc.* **19**, 55-60 (2011).

Reference paper as:

Haff, R., Saranwong, S. and Kawano, S. (2012). Methods for correcting morphological-based deficiencies in hyperspectral images of round objects, in: *Proceedings of the 15th International Conference on Near Infrared Spectroscopy*, Edited by M. Manley, C.M. McGovern, D.B. Thomas and G. Downey, Cape Town, South Africa, pp. 48-51.